# The Principal Axes Transformation—A Method for Image Registration

N. M. Alpert, J. F. Bradshaw, D. Kennedy, and J. A. Correia

*Department of Radiology, Massachusetts General Hospital, Boston, Massachusetts*

We have developed a computational technique suitable for registration of sets of image data covering the whole brain volume which are translated and rotated with respect to one another. The same computational method may be used to register pairs of tomographic brain images which are rotated and translated in the transverse section plane. The technique is based on the classical theory of rigid bodies, employing as its basis the principal axes transformation. The performance of the method was studied by simulation and with image data from PET, XCT, and MRI. It was found that random errors in determining the brain contour are well tolerated. Progressively coarser axial sampling of data sets led to some degradation, but acceptable performance was obtained with axial sampling distances up to 10 mm. Given adequate digital sampling of the object volume, we conclude that registration by the principal axes transformation can be accomplished with typical errors in the range of ~1 mm. The advantages of the technique are simplicity and speed of computation.

**J Nucl Med 1990; 31:1717–1722**

Positron emission tomography (PET) is a nuclear medical imaging technique capable of providing quantitative functional information in intact animals and in human subjects. Because of its functional nature, PET often requires anatomic reference information, obtained on the same subject, to correlate patho-anatomic and functional abnormalities. In addition, it is sometimes desirable to compare serial studies in the same individual. These requirements for anatomic reference information and comparison of repeated measurements has given rise to the technical requirement for image registration, a need most clearly recognized in studies of the human brain whose blood flow and metabolism often exhibit detailed and characteristic patterns, from one individual to another. Currently, the need for image registration has been met with the use of head-holding devices, anatomic markers and, recently, the invention of computer algorithms for after-the-fact image alignment. Head-holding devices, except for the most severe (*1*), do not provide sufficient restraint to ensure exact positional matching. Such devices are also difficult to use across modalities such as computed tomography (CT) and magnetic resonance imaging (MRI) because their use is technically demanding. Anatomic markers have been less widely used, but they too require trained personnel for their use. After-the-fact image alignment implies the application of some computational scheme to bring images into registration, but sufficient three-dimensional data must be available before such procedures can even be contemplated.

It is only recently, when volumetric studies with high enough axial sampling have become available with MRI, CT, and PET, that computational methods for registration have become appealing. One technique, least-squares matching of brain surface coordinates, has already been developed by Pelizzari and colleagues at the University of Chicago (*2–4*). The least-squares method is robust in that some missing or inconsistent data can be tolerated; but nonlinear least squares is an iterative technique often requiring good initial estimates of the parameters for rapid convergence. Sometimes convergence cannot be obtained without human intervention. Analytic techniques have also been proposed, but these require either identification of corresponding landmarks (*5*) or identification of a complete set of points on the surface of the object to be registered (*6,7*).

This paper describes work on an analytic approach, the principal axis transformation, which is appealing because of its computational properties—speed and simplicity. Our goal was to evaluate this technique and to establish its suitability for image registration. A preliminary report on this work was presented in abstract form (*8*), and the principal axis transformation has previously been described by Gamboa-Aldeco and Chen (*6*) and by Faber and Stokely (*9*). Gamboa-Aldeco and Chen focused on applications to treatment planning and Faber and Stokely compared registration of the principal axes to a tensor-based moment method. Our development, originated independently, focuses on registration of XCT and MR data with PET; the theoretical basis is identical but our implementation differs

Received Dec. 18, 1989; revision accepted Apr. 6, 1990.

For reprints contact: Nathaniel M. Alpert, PhD, Division of Nuclear Medicine, Massachusetts General Hospital, Fruit Street, Boston, MA 02114.

from that of Gamboa-Aldeco, who match surfaces rather than volumes.

## THEORY

The principal axis transformation is known from the classical theory of rigid bodies (*10*). A rigid body is uniquely located by knowledge of the position of its center of mass and its orientation (rotation) with respect to its center of mass. The center of mass, inertia matrix, and principal axes can be determined for any rigid body. For simple geometric shapes, the principal axes coincide with the axes of symmetry, and, in general, form an orthogonal coordinate system, with their origin at the center of mass. When computed in the principal axis coordinate system, the inertia matrix is diagonal.

Consider two sets of images in which it is possible to identify corresponding volumes bounded by closed surfaces, but make no assumptions about the orientation or location of these "reference volumes." If the reference volumes represent the same object, the centers of mass, $\vec{R}_i$, $i = 1,2$, of mass will represent the same physical point in the object, independent of orientation or scale. The inertia matrices, $I_i$, for the two reference volumes can be expressed as a similarity transformation:

$$I_i = S_i I S_i^T, \quad (1)$$

where I represents the inertia matrix computed in the principal axis coordinate system; and, the rotation matrix, $S_i$, is the matrix of eigencolumns determined from $I_i$, the eigencolumns are orthonormal vectors directed along the principal axes. Geometrically, Equation 1 can be interpreted as a rotation of the $I$ relative to the original image coordinate axes. $I_1$ and $I_2$ are related by:

$$I_2 = S_2 S_1^T I_1 S_1 S_2^T. \quad (2)$$

Registration of image 1 to image 2 can be obtained by a translation to the center of mass coordinate system followed by the rotation $S_1 S_2^T$.

## METHODS

Assuming the validity of the rigid body assumption, the theory may still be limited in practice by resolution and sampling effects as well as by errors in the specification of the reference volumes. The sensitivity of the method to such errors will determine its practicality in real-world applications. The calculations can be performed on either the surface outlines or filled volumes, but, as will be discussed later, there are reasons to expect the calculations based on outlines to be more sensitive to experimental error. The basic criteria for evaluating the method are the position of the center of mass and rotation of the object about the center of mass, properties which uniquely determine the "location" of a rigid body in three-dimensional space. These experiments were performed with simulated data, PET and CT data sets, and with high resolution, volumetric MRI images of the brain. In the work with image data, we used manual determination of surface outlines, image-by-image, to define the volumes of interest which we refer to as VOIs in analogy to the more common ROI abbreviation. Image sets were treated as rigid bodies with uniform mass density functions.

It is desirable to separate the effects of finite sampling from those due to experimental errors, which are more difficult to control. Two shapes were used to assess the errors resulting from computing the principal axis transformation on a sampled grid. The calculations were performed with both outlines (surfaces) and bit maps (volumes). First, a rhomboid approximating a line 18 cm long (The sampling distances were $\delta x =$ 1 mm, $\delta y = 1$ mm, and $\delta z = 3$ mm) was generated by computer. The longest axis of the rhomboid was aligned parallel to the z-axis and then rotated about its center of mass to known angles (1, 2, 4, 8, 12, 16, and 20 degrees). Second, outlines and bit maps defining the complete cerebral hemispheres on volumetric MRI image sets were rotated in the axial direction about the center of mass by 20°. In each case, the center of mass and angle with respect to the axial direction were compared with the input data.

The effect of random errors was assessed by adding Gaussian random noise to the surface contours of MR data. In this regard, ensembles of noisy data were generated by computer simulation to produce noisy outlines and the corresponding filled volumes. The effect of typical variations in the volume boundary was also checked by performing the calculations on outlines and bit maps determined on MRI data which had been rotated by known amounts, both in-plane and axially.

The effect of variations in slice sampling was studied using a volumetric set of MRI data of the brain. These data ($\delta z$) were resampled to yield slices with slice spacing of 6, 9, 12, and 15 mm.

We tested the method on planar CT and PET data obtained on the same individual where careful axial positioning with a plastic molded head holder determined corresponding slices. Finally, we tested the method on volumetric MR data obtained on the same individual in two different MR scanners on scans acquired one year apart. No a priori attempt was made to align the subject's head in the MR scans. Outlines of the inner table of the skull were drawn on the CT and PET data sets and, outlines of the cerebral cortex were drawn on the two MR data sets. The method was used to obtain the parameters for the translation and rotation needed to register sets 1 and 2 over the cerebral hemispheres. These parameters were used to reposition the CT data over the PET data and, to reslice one of the MR data sets, yielding a new set of images which should, all other things being equal, be registered with the target set.

### Calculations

Centers of mass were computed for the reference volumes and/or their bounding surfaces as:

$$[\bar{x}, \bar{y}, \bar{z}] = Mean\ ([x, y, x]), \quad (3)$$

where $x$, $y$, $z$ are the integer coordinates of an image voxel or surface, the symbol *Mean* indicates the arithmetic mean over the set of reference voxels or surface coordinates, and $\bar{x}$, $\bar{y}$, $\bar{z}$ denote the coordinates of the center of mass.

Transformation to the center of mass coordinate system was performed according to the usual formulas:

$$[x', y', z'] = [x, y, z] - [\bar{x}, \bar{y}, \bar{z}]. \quad (4)$$

The moments and products of inertia were computed as:

$$[I_{xx}, I_{yy}, I_{zz}] = Mean([x'^2, y'^2, z'^2]) \quad (5)$$

$$[I_{xy}, I_{xz}, I_{yz}] = Mean([x'y', x'z', y'z']). \quad (6)$$

### Computer Programs

We developed a set of computer programs, written in FORTRAN-77, to perform the principal axis transformation and to evaluate its performance in image registration. These included programs to compute the center of mass and inertia matrix. A second program, computed the eigenvectors, and, thus, the $S$ matrices, using standard subroutines from the IMSL FORTRAN subroutine library. We imposed additional criteria on the eigenvectors, requiring a right-handed coordinate system, with the positive "z-direction" along the subject's long axis, from foot toward head. Linear interpolation and image scaling, based on the pixel size in the reconstructed images, were used in the image translation and rotation steps.

### Image Data

PET data were gathered with a Scanditronix PC-384 positron camera with three rings of BGO crystals. PET image resolution was 8 mm in-plane and 12 mm axially. Transverse section reconstruction was performed with the filtered backprojection method, producing images of 128 × 128 pixels with dimensions of 2.55 $mm^2$. A General Electric 8800 scanner (Milwaukee, WI) was used to perform XCT studies. Reconstructed XCT images were acquired in the medium resolution body mode producing reconstructed images with a pixel size of 1.95 mm and a slice thickness of 10 mm. The same individually molded plastic-foam headholder was employed for both PET and CT scan sessions to define corresponding slices. We acquired three-dimensional volumetric MR image data of a volunteer on two occasions, one year apart, on scanners at different locations. In each case, we used a Siemens Magnetom 1.0 Tesla imaging system (Des Plaines, IL). The image acquisition performed was a coronal FLASH sequence with repetition time 40 msec, echo time 15 msec, pulse angle 50°, and matrix size 256 × 256 × 63 with in-plane spatial resolution of 1.17 mm and a contiguous slice thickness of 3.125 mm.

## RESULTS

### Effect of Sampling Grid

Small effects, generally negligible, can be ascribed to digital sampling. Rotation of a the test rhomboid (approximating a line 18 cm long) line as described above had no effect on the computation of the center of mass. The difference between intended and computed rotation angle varied from 0.05°–0.48°. When the calculations were performed on bit maps and outlines (determined on NMR data of the human brain) which were rotated 20.0°, the position of the center of mass varied by less than 0.005 mm; and the rotation angle differed by 0.16°. To put these results in perspective, the maximum positional error due to misrotation of 0.5° for a point 100 mm from the center of mass is given approximately by $r\Delta\theta = 0.9$ mm.

Calculations made using surface outlines were more sensitive to random noise in the boundary determination than were those using volumes. The effect of noise on calculations using surfaces and volumes is shown in Figures 1 and 2. Figure 1 shows the RMS error in position (translation error) of the center of mass as a function of noise added to the surface outlines determined on NMR images. Similarly, Figure 2 shows the RMS error in rotation about the "z" principal axis as a function of Gaussian random noise in the contours. The calculations show translational and rotational errors are three to six times greater for registration using surfaces rather than volumes. Similarly, when surfaces were redrawn on data sets rotated by known angles the errors using bit maps (volumes) were much smaller. For example, after 20-degree axial rotation and redrawing of the surfaces to simulate typical experimental error, the calculation on bit maps resulted in an error of 1.2°, whereas the calculation on the outlines differed by 8.4°.

The effect of increasing the axial sampling distance on location of the center of mass and rotational error is shown in Figures 3 and 4, respectively. At the largest sampling distances, there are more unique ways of sampling the object and this is reflected in the figures by the increasing number of points plotted. As expected, the error due to missing samples increases with the sampling distance. At 3 mm sampling distance, removing every other sample had negligible effect; but at a sampling distance of 15 mm the error in the location of the axial component of the center of mass can be as much as 0.5 mm and the rotation error (axial) was as

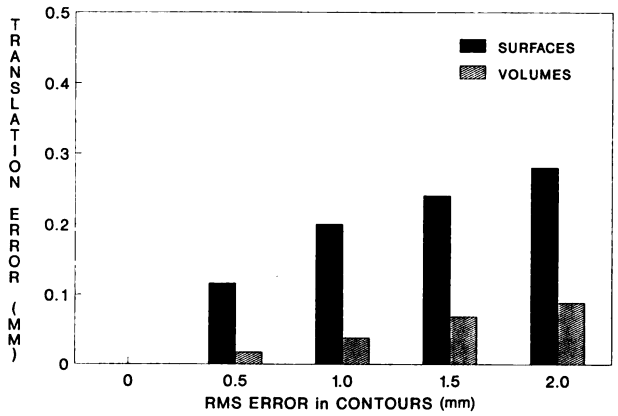


**FIGURE 1**
RMS error in the location of the center of mass (translation error) of a volumetric set of MR brain images. Simulations were performed by adding Gaussian distributed noise to the original cerebral outlines. The noise was added to each point within the xy-plane of the original outline in a radial direction from the center of mass to simulate error in the drawing of the outlines. Each plotted value represents 100 noise runs.

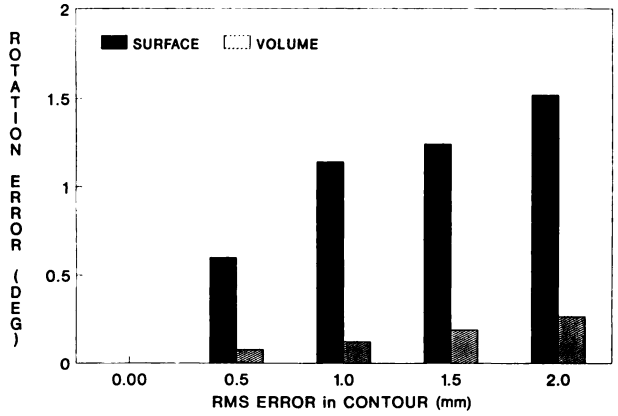


**FIGURE 2**
RMS error in the rotation angle (rotation error) of a volumetric set of MR brain images. Simulations were performed using the same noisy outlines as in Figure 1. The principal axis transformation determined the rotation about the "z" eigenvector. Each value represents 100 noise runs.

much as 1°; and the maximum errors were even larger for sampling distances >15 mm.

Examples of image registration, obtained by the principal axis transformation, are shown in Figures 5 and 6. Figure 5 illustrates use of the method to refine the localization provided by a molded plastic headholder. It was assumed that the axial position was determined by the headholder, but that the position and rotation of the slice could vary within the plane. Figure 6 shows the results of applying the method to two sets of MR data obtained on the same individual using different MR scanners without any a priori attempt to match head position. It is interesting to note in Figure 6 that only the cerebral hemispheres and cerebellum appear to be registered. This is because the rigid body assumption fails outside the brain.

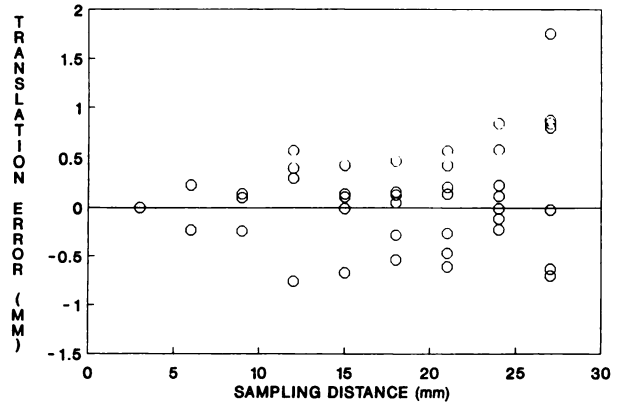


**FIGURE 3**
Translational error in the computed axial (z) component of the center of mass of an MR image for progressively coarser axial (z) sampling. The original data are sampled with 3-mm slice thickness. Samples were then removed and the resultant z-position shift plotted. Each point represents a different set of samples at the indicated sampling distance.

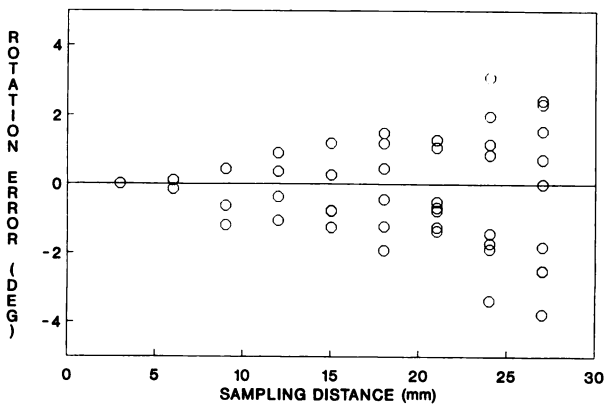


**FIGURE 4**
Rotational error in the computed angle of the "z" principal axis of an MR image for progressively coarser axial (z) sampling. The samples are the same as those in the previous graph. Each point represents a different set of samples at the indicated sampling distance.

## DISCUSSION

We have developed a computational technique suitable for registration of pairs of tomographic brain images that are rotated and translated in the transverse section plane or for pairs of image sets covering the whole brain volume. The validity of the approach hinges on the assumption that the brain does not deform, or move within the cranium, when imaged in different orientations. But Talairach et al. (*11*) in their carefully performed studies, using stereotactic methods and the superimposition of pneumoencephalograms, were unable to detect deformations or movements.

A theoretical limitation of the method arises when aligning objects with a high degree of symmetry, as for example, spheres or regular polyhedrons; symmetries may result in eigenvector solutions which are not unique. Such limitations are not likely to be of practical significance in medical applications.

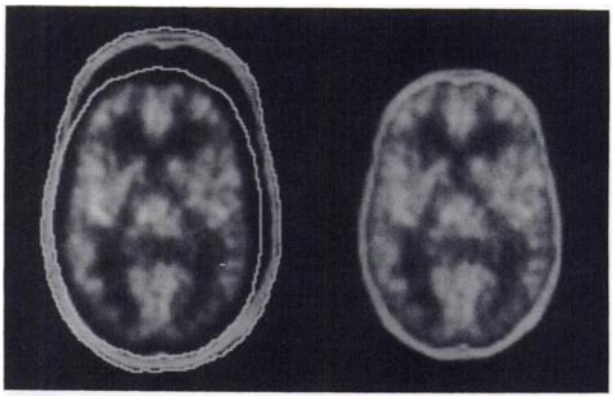

**FIGURE 5**
Alignment of a PET and CT scan on the same patient within the transaxial (x-y) plane. Axial (z) alignment was done externally with a head holder. One combined PET and CT slice is shown before (left) and after (right) alignment. In addition to the coordinate transformation, the CT image is scaled.

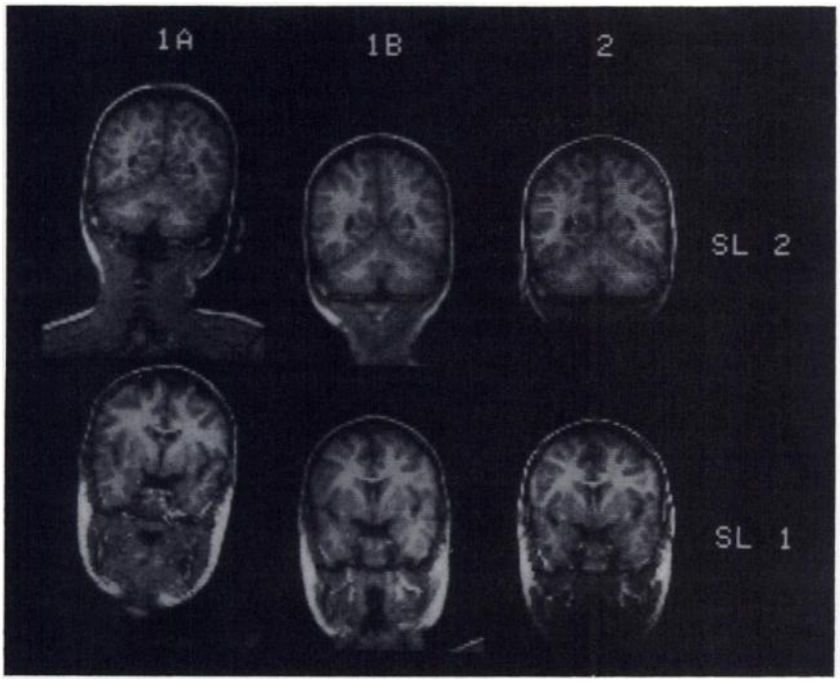


**FIGURE 6**
Illustration of a three-dimensional registration of two volumetric MR scans of the brain. The scans were performed on the same subject, using two different MR scanners. The time interval between scans was ~1 yr. Two slices are shown, SL1 and SL2. The data in column 1 were chosen visually, from a completely sampled volumetric set (see text), to roughly correspond to the data from the second scan session (column 2). Column 3 illustrates the result of the principal axes registration of set 1 to set 2, providing visual confirmation of the alignment.

We noted above that the boundaries of the volumes to be registered were delineated manually. The need for such segmentation prior to registration is common to all surface and volume matching algorithms described to date. However, it should be noted that a variety of automatic and semiautomatic image segmentation algorithms have been described.

Studies with the principal axis transformation have been used to align PET and CT studies in two dimensions and MRI data in three dimensions. Since the registration is analytic, requiring only computations of moments and matrix inversion, it offers advantages of speed and simplicity over iterative methods such as least squares. Calculation of the moments and the principal axis transformation requires ~2 min on a Digital Equipment Corp (Maynard, MA) VAX-11/780 computer with no special arthimetic acceleration hardware. The quality of the registration appears to be limited by two factors: (1) the three-dimensional sampling of the volume by the imaging device; and (2) the ability to delineate exactly corresponding volumes in the two image sets. Even so, we conclude that it is possible to achieve registration of brain data in which typical errors will be ~1 mm.

Because of a lack of suitable volumetric PET and MRI data in the same subject, we were unable to directly verify registration between PET and MRI. However, registration between volumetric MRI data sets was such that the data were essentially indistinguishable, raising the practical question, how good a registration do we need? Data gathered in our laboratory for a PET camera with 8 mm in-plane and 12 mm axial resolution indicates that a 2.5-mm in-plane shift between cerebral blood flow studies results in an average error of 2 ml/min/100 g and a worst case error of 10 ml/min/100 g. Such errors are barely tolerable and would presumably be worse with higher tomographic resolution. So, registration should ideally be better than 2 mm in all directions.

The work by Englestad and his colleagues (*7*) is related to this work in that it uses the first and second moments of image ROIs. Engelstad et al. assume that the surface of the brain or skull can be approximated by an ellipse and use the center of mass and the second moments to compute the equation of the ellipses for corresponding slices. These equations determine the in-plane translation and rotations needed for registration in two dimensions. Their work can be seen as a special case of the principal axis transformation, which makes it unnecessary to assume an approximating geometric shape such as an ellipse. Furthermore, their technique could, in principal, be extended to three dimensions; the derivation of the enalogous three-dimensional equations assume an ellipsoid of revolution, and could achieve equivalent results at the cost of tedious, brute force algebraic manipulation.

We noted earlier that Gamboa-Aldeco and Chen (*6*) have also studied the principal axis transformation for image registration. Their paper is noteworthy for an elegant derivation of the theory. However, it should be pointed out that their implementation employed the surface elements bounding the volume rather than the volume elements themselves. Theoretically, the surface elements contain all the information necessary for computing the principal axes. However, consideration of the effect of noise on the moments and products of inertia as well the direct comparisons reported here suggest that use of all the volume elements in the

computation produces a result which is less sensitive to systematic and random errors.

It is possible to suggest a relationship between least-squares techniques and this work. Froimowitz and Matthysse (*12*) compared the conformation of the tyrosine portion of the enkephalins and morphine-like opiates by computing the minimum RMS distance between the conformers. They showed for two rigid bodies $K$ and $K'$, each composed of $N$ points internally connected, that the minimum sum of the squares distance between *corresponding points* is achieved by a calculation equivalent to the principal axis transformation.

Computational approaches to image registration have a practical advantage over methods which rely on anatomic markers or protocols which attempt to select slices which correspond exactly. The advantage is improved technical feasibility, lessening the demands on personnel to use special headholders or to affix anatomic markers. Making a choice among the computational techniques depends on a number of factors that have not been completely studied. For example, it is expected that least-squares will be robust against errors due to data with random errors, but since it depends on iterative, nonlinear parameter estimation methods, convergence problems may result from missing or inconsistent data. On the other hand, the principal axes method is analytic, and, hence, does not suffer from convergence problems, but is likely to be more vulnerable to missing data. Prospective users should prefer the least-squares approach if missing data (e.g., an incompletely sampled hemispheric volume) are likely to occur in their imaging procedures. Otherwise, the principal axes method offers advantages in speed and simplicity.

## REFERENCES


1. Bergstrom M, Boethius J, Eriksson L, Greitz T, Ribbe T, Widen L. Head fixation device for reproducible position alignment in transmission ct and positron emission tomography. *J Comp Assist Tomgr* 1981; 5:136–141.
2. Pelizzari CA, Chen GTY, Spelbring DR, Weichslebaum. Accurate three-dimensional registration of CT, PET and/or MR images of the brain. *J Comput Assist Tomogr* 1989; 13:20–26.
3. Chen CT, Pelizzari CA, Chen GTY, Cooper MD, Levin DN. Image analysis of PET data with the aid of CT and MR. In: DeGraff CN, Viergever MA, eds. *Information processing in medical imaging.* London: Plenum Press; 1988:601–611.
4. Levin DN, Pelizzari CA, Chen GTY, Chen CT, Cooper MD. Retrospective geometric correlation of MR, CT and PET images. *Radiology* 1988; 169:817–823.
5. Marret S, Collins L, Evans A. A tool for volumetric PET/MRI image matching and display [Abstract]. *J Nucl Med* 1989; 30:776.
6. Gamboa-Aldeco A, Chen GTY. Correlation of 3D surfaces from multiple modalities in medical imaging. *SPIE proceedings* 1986:460–466.
7. Englestad BL, Meyers HJ, Hanson WA, O'Connell JW, Taylor RC, Bernstein R. Information extraction from multimodality medical imaging. In: *Three-Dimensional imaging and remote sensing.* SPIE; 1988:144–149.
8. Alpert NM, Bradshaw J, Senda M, Correia JA. The principal axis transformation: a method for image registration [Abstract]. *J Nucl Med* 1989; 30:776.
9. Faber TL, Stokely EM. Orientation of 3-D structures in medical images. *IEEE Trans Pat Anal and Mach Intel* 1988; 10:626–633.
10. Goldstein H. *Classical mechanics.* Reading, MA: Addison Wesley; 1959.
11. Talairach J, Szikla G. *Atlas of stereotactic anatomy of the telencephalon,* Paris: Masson and Cie; 1976.
12. Froimowitz M, Matthysse S. Geometrical correspondence between phenazocine and the enkephalins. *J Med Chem* 1986; 29:573–578.